Journal of the American Association for Laboratory Animal Science
Copyright 2013
by the American Association for Laboratory Animal Science

Vol 52, No 5
September 2013
Pages 545–552

Immunopathologic Characterization of Naturally Acquired *Trypanosoma cruzi* Infection and Cardiac Sequalae in Cynomolgus Macaques (*Macaca fascicularis*)

Harshan Pisharath,[1,*] Chih-Ling Zao,[3] John Kreeger,[2] Susan Portugal,[2] Thomas Kawabe,[2] Tarea Burton,[3] Lisa Tomaeck,[3] Ahmed Shoieb,[2] Brandy Morenko Campbell,[1] and Judy Franco[1]

***Trypanosoma cruzi*, the causative agent of Chagas disease, is endemic in south Texas due to the abundant vector and wild small mammalian reservoir populations. This situation predisposes nonhuman primate colonies exposed to outdoor housing to infection from ingestion or bite of triatomid insects. Using a *T. cruzi*-specific real-time PCR and *Trypanosome* spp.-specific ELISA, we revealed a prevalence rate of 8.5% in a colony of outdoor-housed cynomolgus macaques. By using a discriminating kinetoplastid minicircle PCR, we eliminated the possibility of mixed prevalence with nonpathogenic trypanosomes and showed the ELISA results were specific for *T. cruzi*. In this study, we found an inverse relationship between antibody titers and circulating parasite load. Also, 23% of *T. cruzi* IgG ELISA-positive macaques were negative by real-time PCR. Furthermore, in a subset of infected macaques, cardiac tissue was infiltrated by inflammatory mononuclear cells and contained *T. cruzi* genomic and kinetoplast DNA despite lacking microscopic evidence of discrete parasite stages. In addition, 19% of the infected macaques had titers for cardiac troponin I autoantibody, which could contribute to autoimmune myocarditis or interfere with circulating troponin I measurements. These findings indicate the possibility of *T. cruzi* to interfere with the assessment of cardiac safety signals in preclinical toxicology and safety pharmacology studies and the necessity for prestudy screening for *T. cruzi* in outdoor-housed nonhuman primates from endemic areas.**

Trypanosoma cruzi, a kinetoplastid protozoan, is the causative agent of Chagas disease.[4,11] In humans, initial infection with *T. cruzi* results in an acute-phase peripheral parasitemia that presents with nonspecific clinical signs, which are followed by a symptom-free indeterminate period. This symptomless period marks the chronic phase of the disease, during which the parasite persists indefinitely within host cells by evading the immune system. A subset of infected patients develops chronic disease, which is characterized by cardiac, gastrointestinal, or nervous system involvement.[15] Like humans, dogs and nonhuman primates also manifest the cardiac form of the disease, developing progressive inflammation leading to myocarditis and fibrosis and dysfunction of the cardiac autonomic ganglia.[1,7,9,12,19]

The epimastigote stages of *T. cruzi* are carried in the guts of hematophagous triatomids, with transmission to mammalian hosts occurring when bite sites or mucous membranes are contaminated by metacyclic trypomastigotes in the insect feces.[4,19] In addition, transfusion–transplantation-related and transplacental congenital infections can occur and are important nonvector routes of transmission.[4,17,23,32] Oral transmission due to ingestion of food contaminated with vector feces and urine or paracloacal secretions of infected marsupials is gaining importance in various regions of South America.[22,29]

Chagas disease is a serious public health concern in many areas of Latin America and Mexico. Although vector-transmitted human cases are rare in the United States, *T. cruzi* is endemic in south Texas because an autochthonous domestic and peridomestic cycle exists due to abundant triatomid vector population and vertebrate reservoirs like woodrats, raccoons, and opossums.[21] This ecologic risk can predispose nonhuman primates housed in outdoor or semioutdoor facilities to infection from bites or ingestion of vector, with the associated cardiac sequelae. There have been reports of heart disease consistent with Chagas myocarditis and cardiomyopathy in Old World species housed in outdoor enclosures at primate centers in the southern United States or experimentally infected with *T. cruzi*.[1,8,9,31] Our initial screening of cynomolgus macaques held at vendor colonies in south Texas by using *T. cruzi* IgG ELISA and real-time PCR of peripheral blood disclosed a combined prevalence of 8.5%. Coupled with the lack of a confirmation assay for routine colony screening and difficulty in microscopic identification of tissue stages of the parasite in cardiac inflammatory lesions, this prevalence may lead to the incorrect attribution of such findings to the drug molecule in pharmaceutical development preclinical safety studies. On the same note, the potential to induce cardiac arrhythmia subsequent to autonomic dysfunction in safety pharmacology studies, polyclonal immune stimulation by parasitic antigens to interfere with immunotoxicologic assays, parasite reactivation to cause myocarditis and encephalitis in immunomodulatory–immunosuppression studies, and the concern for transplacental infection of fetus to compromise pre- and postnatal developmental safety studies can adversely affect drug candidate selection and decisions regarding late-stage (phases 2 and 3) development. In light of this effect on scientific endpoints and study outcomes, we sought to character-

Received: 25 Jan 2013. Revision requested: 03 Mar 2013. Accepted: 30 Apr 2013.
[1]Worldwide Comparative Medicine and [2]Drug Safety R&D, Worldwide R&D, Pfizer, Groton, Connecticut; [3]VRL Laboratories, San Antonio, Texas.
[*]Corresponding author. Email: harshan.pisharath@nationwidechildrens.org

ize concordance between serology and peripheral blood parasite load by using *T. cruzi* IgG and IgM ELISA and *Taq*Man-based real-time PCR assay to validate a prestudy screening strategy. Using an ELISA method, we studied total circulating IgG levels as a marker of parasite-antigen–induced polyclonal B-cell activation, which is linked to the production of polyantigen-reactive autoantibodies.[5,18] We also assessed circulating autoantibody titer against cardiac troponin I in *T. cruzi*-positive and -negative cynomolgus macaques to shed light on parasite-induced autoimmunity and its role in cardiac pathology. Such autoantibodies could also interfere with many preclinical endpoint assays, like serum troponin I measurement for cardiac safety. Using immunohistochemistry, we characterized the inflammatory infiltrate in cardiac lesions in *T. cruzi*-positive macaques and showed that although they lacked identifiable tissue stages of the parasite, these tissue sections contain detectable levels of trypanosomatid nuclear and kinetoplastid DNA.

Materials and Methods

Animals. Purpose-bred Mauritian-sourced cynomolgus macaques (*Macaca fascicularis*) were housed at an AAALAC-accredited contract holding facility in Alice, TX. Animals used in this study are SPF for B virus (*Macacine herpesvirus* 1), simian T-lymphotropic virus 1, SIV, and simian retrovirus type D (serogroups 1 through 5) and are periodically tested and found to be negative for tuberculosis. The blood-collection procedures were performed in conformance with IACUC protocols and standards. Macaques were 5 to 6 y old and were housed exclusively indoors during the quarantine period and subsequently transferred to indoor–outdoor runs that held 10 to 15 animals each. Macaques were housed in indoor–outdoor enclosures (potential risk factor for acquiring *T. cruzi* infection) for 22 to 31 mo (average, 28 mo). For this study (August 2012), 84 animals were bled for serum and whole blood. In addition, all 84 macaques had been tested at least twice by PCR and ELISA between 1 and 4 mo prior to the study sampling date as part of colony-wide screening, the results of which were used to select animals for the current study.

Histopathologic studies in Mauritian-sourced cynomolgus macaques that originated from suppliers that housed animals in indoor–outdoor runs or outdoor enclosures exclusively in south Texas were conducted at an AAALAC-accredited facility and IACUC-approved. Cardiac tissue from 8 macaques identified as *T. cruzi*-positive according to PCR and ELISA screening were used for histologic, tissue PCR, and immunohistochemistry studies.

Histology. Formalin-fixed whole hearts were processed for histopathologic evaluation. Sections of the right and left atria and ventricles and basal and apical portions of the interventricular septum were trimmed for further processing. Paraffin-embedded tissue was processed for slides and underwent routine hematoxylin and eosin staining and immunohistochemistry. The slides were evaluated by board-certified veterinary pathologists.

Immunohistochemistry. Paraffin-embedded formalin-fixed heart sections were stained for B cells, T-helper and T-cytotoxic cells, and macrophages by using the following antibodies and protocols. B cells were incubated with CD20 Bond Ready-To-Use Primary antibody (proprietary dilution; clone MJ1, Leica Biosystems, Richmond, IL) by using the Leica Bond III automated stainer and the Refine Polymer Kit (Leica Biosystems). T-helper cells were stained by using Novocastra antiCD4 (diluted 1:50; clone 1F6, Leica Biosystems). Immunohistochemical localization for CD4 was done by using the Discovery XT UltraMap antiMS AP Immunohistochemistry Protocol (Ventana Medical Systems, Tucson, AZ). T-cytotoxic cells were stained by using Novocastra CD8 antibody (diluted 1:50; clone1A5, Leica Biosystems); bound antibody was visualized by using heat-induced epitope retrieval with EDTA in a Decloaking Chamber (Biocare Medical, Concord, CA). Macrophages were stained by using Novocastra antibody CD68 (diluted 1:250; clone KP1, Leica Biosystems), followed by heat-induced epitope retrieval with Citra (BioGenex, Fremont, CA) to localize the CD68 antibody. Bound antiCD8 and antiCD68 were detected by using intelliPATH FLX (Biocare Medical) and Envision+ Mouse HRP (Dako, Carpinteria, CA). All slides were counterstained by using Mayer hematoxylin (Dako). Appropriate positive controls for the antibodies used were run concurrently with test samples and showed appropriate immunostaining. Negative-control sections were processed without the primary antibody.

Absolute quantitative real-time PCR assay. DNA was extracted from EDTA-treated whole blood by using the Generation Capture Column Kit (Qiagen, Valencia, CA) according to the manufacturer's protocol and was amplified in a model 7300 Real-Time PCR System (Applied Biosystems, Foster City, CA). Plasmid standards containing *T. cruzi* nuclear satellite DNA and an endogenous reference gene (GAPDH) were synthesized (GenScript, Piscataway, NJ) and included in each 96-well plate run. The DNA template (500 ng per reaction) was added to *Taq*Man Gene Expression Master Mix (Applied Biosystems) containing *T. cruzi*- and GAPDH-specific primers and probes in each PCR reaction according to standard protocol (VRL Laboratories, San Antonio, TX). This PCR assay specifically amplified *T. cruzi* nuclear repetitive satellite sequences and did not detect nonpathogenic *T. rangeli*. The copy number of the *T. cruzi* target gene or GAPDH in the samples was calculated according to a standard curve method using the plasmid standards. GAPDH values were used to normalize *T. cruzi* copy numbers to estimate circulating parasite loads, which are expressed as the ratio of $\log_{10}$ (*T. cruzi* copy number) / $\log_{10}$ (GAPDH copy number).

***Trypanosoma* spp. minicircle PCR assay.** DNA was extracted from EDTA-treated whole blood by using the Generation Capture Column Kit (Qiagen) according to the manufacturer's protocol. DNA from formalin-fixed, paraffin-embedded tissue samples was extracted by using the PureLink Genomic DNA kit (Invitrogen, Carlsbad, CA) according to the manufacturer's protocol, except that Histochoice Clearing Agent (Sigma Aldrich, St Louis, MO) was substituted for Citrisolve (Fisher Scientific, Fair Lawn, NJ) to dissolve paraffin. To distinguish between *T. cruzi* and nonpathogenic *T. rangeli*, primers S35 and S36 were used to differentially amplify *T. cruzi* and *T. rangeli* kinetoplast DNA minicircles[30] in a model 2720 thermocycler (Applied Biosystems). PCR products were electrophoretically separated in a gel containing 1.5% UltraPure Agarose (Invitrogen) and stained with ethidium bromide (Invitrogen). A sample containing *T. cruzi* DNA is expected to yield a 300- to 330-bp DNA band, and *T. rangeli* is expected to yield a 760-bp DNA band as well as several other bands varying from 300 to 450 bp.

Chagas IgG and IgM ELISA. Whole-organism lysates of *T. cruzi* (epimastigote antigens) were used to coat 96-well ELISA plates, which then were blocked with 1% BSA (KPL, Gaithersburg, MD). Serum samples were prediluted to 1:26 in 1% BSA for use in Chagas IgG ELISA; serum samples were pretreated with GullSorb (Meridian Bioscience, Cincinnati, OH) and brought to a final dilution of 1:200 for Chagas IgM ELISA use. Diluted serum samples were transferred to the ELISA plates and incubated at room temperature for 30 min. After the wells were washed, antihuman IgG or antihuman IgM peroxidase-labeled conjugate

(KPL) was added to each well and incubated at room temperature for 30 min; 3,3′,5,5′ tetramethyl benzidine then was used to develop color and 1 N H_2SO_4 was used to stop the reaction. The plate was read at 450 nm by using the ELx800 plate reader and using KC Junior software (both from BioTek).

Antitroponin I IgG autoantibody ELISA. Human cardiac troponin I (Life Diagnostics, West Chester, PA) antigen was coated on 96-well ELISA plates and blocked with 1% BSA (KPL). Serum samples were diluted 1:50 in 1% BSA before being transferred to the ELISA plates. After incubation at room temperature for 2 h, the samples were discarded, and plates were washed. Antihuman IgG peroxidase conjugate (KPL) was added to each well and incubated at room temperature for 1 h. After being washed, TMB substrate (KPL) was added for color development, and 1N H_2SO_4 was used to stop the reaction. The OD_{450} of each plate was read (ELx800, BioTek, Winooski, VT); OD_{450} values were normalized between plates by using high- and low-titer sera. Samples with OD_{450} values at or above the mean + 3SD of the *T. cruzi*-negative group were used as a cut-off for reporting the proportions of macaques with circulating antitroponin I autoantibodies within groups.

Total IgG ELISA. Macaque IgG was quantified by using a monkey IgG ELISA kit (Alpha Diagnostics, San Antonio, TX). Serum samples were diluted in a 3-step process to a final dilution of 1:400,000, according to the manufacturer's protocol. Briefly, wells were washed with Working Buffer Solution (Alpha Diagnostics) and incubated for 5 min. The wells then were aspirated according to manufacture protocol and patted dry. Samples, controls, and standards were added at 100 µL per well and incubated 60 min. The wells were washed 4 times with Working Buffer Solution (Alpha Diagnostics) and patted dry. Each well then received 100µL of diluted antimonkey IgG horseradish peroxidase conjugate and incubated 30 min. The wells were washed 5 times with Working Buffer Solution (Alpha Diagnostics) and patted dry. Each well then received 100 µL TMB substrate (Alpha Diagnostics) and incubated in the dark for 15 min, according to the manufacturer's protocol. Once developed, each well then received 100 µL of Stop Solution supplied with the kit. The plate was read within 30 min at 450 nm (ELx800, BioTek) by using KC Junior software (BioTek). If the OD_{450} values were out of range (that is, exceeded 3.0), samples were prediluted 1:2 and then the 3- step dilution was completed according to manufacturer's protocol. The final total IgG concentration was calculated by determining the average OD_{450} of each sample against the standard (in ng/mL) after compensating for background. Quantities were adjusted for the dilution factor and converted to values in mg/mL.

Statistics. Association between assays was tested by using the Fisher exact test for 2×2 contingency tables. The means of the total circulating IgG of *T. cruzi*-infected and -uninfected groups were compared by using the Student *t* test. All statistical tests and plots were done by using SAS for Windows version 9.2 (SAS Institute, Cary, NC).

Results

PCR- and ELISA-based detection of *T. cruzi* We used real-time PCR to identify *T. cruzi*-specific nuclear mini-satellite DNA sequences and ELISA to detect antitrypanosomal IgG in 84 cynomolgus macaques at risk (exposure to outside in an endemic area) for *T. cruzi* infection (Table 1). Among the 84 macaques, 39 were previously deemed *T. cruzi*-positive and the remaining 45 were *T. cruzi*-negative according to PCR and ELISA screening in March, May, or June 2012. Subsequently, 4 of the 45 previously negative animals were positive by PCR and ELISA during the current (August 2012) testing, indicating an incidence rate of 9% for this time period. Of the 43 samples previously identified as positive by IgG ELISA, 10 (23%) were deemed negative by real-time PCR. Despite this incongruity, there was a statistically significant (Fisher exact test, $P < 0.001$) association between real-time PCR and IgG ELISA results. When the real-time PCR results were compared with screening (PCR and ELISA) data that had been obtained from the same group of animals approximately 2 to 3 mo prior to the current sampling (data not shown), 3 macaques deemed negative continued to remain so, but 7 macaques previously deemed positive had turned negative. This pattern could suggest either intermittent parasitemia or a circulating parasite load falling below the threshold for detection. Because *T. cruzi* causes life-long infection of tissues, we do not believe that these cases represent clearance of parasite.

We identified a statistically significant negative correlation ($r = -0.49$; $P = 0.002$) between circulating parasite load and anti*T. cruzi* IgG titer (Figure 1). This analysis also identified a strong association between high anti*T. cruzi* IgG titer and negative real-time PCR results.

To better characterize the serologic response and correlation to circulating parasite levels, we modified the IgG ELISA procedure to detect serum anti*T. cruzi* IgM levels in this population. We used the macaques that were negative by real-time PCR and IgG ELISA to establish cut-off levels for the IgM assay. Applying this assay separately to the groups positive by real-time PCR and IgG ELISA (Tables 2 and 3) failed to reveal any significant association (Fisher exact test $P = 0.08$; Fisher exact test $P = 0.36$).

Because the real-time PCR for nuclear minisatellite DNA is specific for *T. cruzi*, we used a generic PCR assay for detecting kinetoplast minicircle sequences on whole-blood DNA extracts from pooled samples of 4 or 5 individual macaques per PCR tube to identify the presence of nonpathogenic trypanosomes, such as *T. rangeli.* When the minicircle DNA primers are used, samples containing *T. cruzi* DNA are expected to yield a 330-bp DNA band, whereas *T. rangeli* is expected to yield a 760-bp DNA band along with several other bands varying from 300 to 450 bp. All of the 7 pooled samples yielded amplicons at 300 or 330 bp and are therefore infected only with *T. cruzi*; none of the samples yielded amplicons at 760 bp (Figure 2). The low-intensity bands at 500 bp in some samples were sequenced and identified as nonspecific amplification from macaque host DNA genome (data not shown).

***T. cruzi*-induced myocarditis.** Given the propensity for *T. cruzi* to induce myocarditis and cardiomyopathy, 8 macaques identified positive by *T. cruzi* IgG ELISA (all 8 macaques) or real-time PCR (5 of the 8) were evaluated histopathologically for the presence of cardiac lesions; 2 animals were normal whereas the remaining 6 had mild to moderate multifocal areas of inflammatory infiltrates that were composed mainly of mononuclear cells with fewer neutrophils and was associated with few degenerate and necrotic myocardiocytes (Figure 3 A and B). On immunohistochemistry, the mononuclear cells were predominantly CD8- and CD68-positive with fewer CD4-positive lymphocytes (Figure 3 D through F), indicating an inflammatory phenomenon. The cardiac basal autonomic ganglion in one infected macaque that was not part of this cohort was infiltrated with mild inflammatory mononuclear cells (Figure 3 G). Unlike intracellular amastigotes of *T. cruzi* (Figure 3 A; notice that the area is devoid of inflammation), areas of inflammation were microscopically negative for discrete parasitic forms, consistent with the notion that inflammation and cell damage are triggered by parasitic replication and an antiparasite immune response to extracellular forms. We performed real-time PCR and minicircle

Table 1. Association between real-time PCR and anti*T. cruzi* IgG ELISA

	Anti*T. cruzi* IgG ELISA	
Real-time PCR	Positive	Negative
Positive	33	0
Negative	10	41

Fisher's exact test of independence, $P < 0.001$.

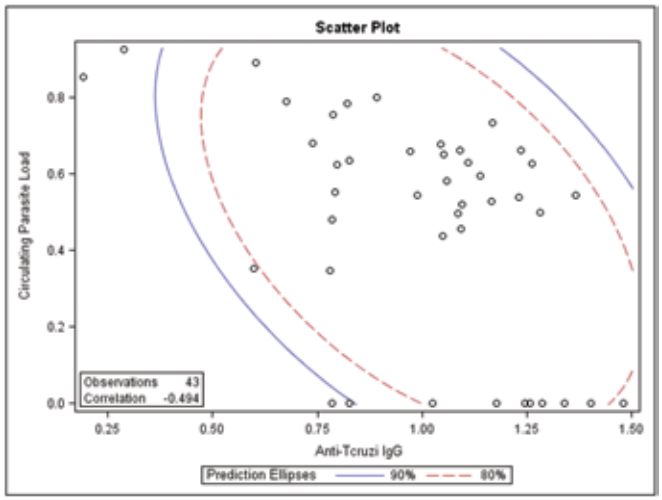

Figure 1. Correlation ($P = 0.002$) between circulating parasite load (expressed as the ratio of the log of absolute copy number of *T. cruzi* nuclear satellite DNA to that of GAPDH) with anti*T. cruzi* IgG titer expressed in OD units.

Table 2. Association between real-time PCR and anti*T. cruzi* IgM ELISA

	Anti-*T. cruzi* IgM ELISA	
Real-time PCR	Positive	Negative
Positive	4	29
Negative	1	50

Fisher's exact test of independence, $P = 0.08$.

conventional PCR assays on adjacent sections from these tissue blocks and found that all 8 of these samples were positive for *T. cruzi* nuclear minisatellite DNA (data not shown), highlighting the limitation of histology for etiopathologic characterization of inflammatory lesions.

Anticardiac troponin I autoantibodies in *T. cruzi*-infected macaques. Cardiac inflammatory lesions in *T. cruzi*-infected macaques and the reports of autoimmunity in infected humans[25,27] prompted us to explore the possibility of circulating autoantibodies against cardiomyocyte proteins in infected macaques. We screened the *T. cruzi*-positive and -negative cohorts to characterize their anticardiac troponin I autoantibody titer levels. Using an ELISA method, we identified 8 of 43 (19%) infected macaques to have circulating autoantibody titers against cardiac troponin I. These levels were significant (Fisher exact test, $P = 0.01$) compared with the lack of titer (0 of 41 macaques with anticardiac troponin I antibodies) in the *T. cruzi*-negative group (Table 4).

Total circulating IgG levels in *T. cruzi*-infected macaques. Polyclonal B cell activation is a recognized phenomenon during *T. cruzi* infection and is thought to play a role in the generation of polyantigen-reactive autoantibodies.[18] We therefore screened *T. cruzi*-positive and -negative cohorts by using a macaque IgG-specific ELISA. Compared with the uninfected group, infected macaques had significantly (*t* test, $P = 0.041$) higher levels of total circulating IgG (Figure 4; mean difference, 7.01 mg/mL; SE, 3.38 mg/mL).

Table 3. Association between anti*T. cruzi* IgG ELISA and anti*T. cruzi* IgM ELISA

	Anti-*T. cruzi* IgM ELISA	
Anti*T. cruzi* IgG ELISA	Positive	Negative
Positive	4	39
Negative	1	40

Fisher's exact test of independence, $P = 0.36$.

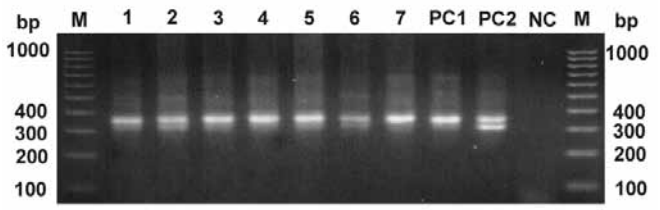

Figure 2. Kinetoplast minicircle DNA detection by PCR. A 300- or 330-bp fragment (or both) amplified from *T. cruzi* minicircle DNA was present in all tested samples. M, DNA ladder marker (bp); lanes 1 through 7, pooled DNA pool samples (each pool contained 4 or 5 individual DNA samples that had been previously tested positive in *T. cruzi* real-time PCR); positive controls showing 330 bp (PC1) and 300- and 330-bp bands (PC2); nc, negative control (no-template control).

Discussion

We used antitrypanosome IgG ELISA and *Taq*Man-based real-time PCR to screen a group of cynomolgus macaques at risk for infection via outdoor exposure in south Texas, where Chagas disease is endemic. An initial screening of an overlapping population larger than what was screened in the current study established a prevalence rate of 8.5% over a period of 24 to 28 mo. In the current study, retesting of 45 negative macaques at risk established an incidence of 9% in the span of 2 to 3 mo (June through August). Seasonal variations in disease transmission rates due to vector- and parasite-related ecologic factors are possible.

In the current study, we identified 10 macaques that were negative by real-time PCR for parasitemia but positive by *T. cruzi* ELISA; 7 of these 10 animals were previously positive by real-time PCR, revealing the limitations of this assay due to either the intermittent nature of parasitemia or to falling of the parasite load below the level of detection. We used 5 mL blood for DNA extraction and applied 500 ng DNA per PCR tube. Given this sensitivity for detection, we believe that either circulating parasites are sequestered or parasite release is suppressed by the immune system through rising antibody titers. We base this argument on the negative correlation between blood parasite load and IgG titer, with a unique subgroup with high titers in the absence of circulating parasites (Figure 1). Previous to the current study, we applied these 2 assays to 100 *T. cruzi*-free cynomolgus macaques housed exclusively indoors to reveal 100% specificity. This result is not surprising for the PCR assay, because the primers and probe target *T. cruzi*-specific nuclear sequences. However, the *T. cruzi* ELISA is nonspecific, because the coated *T. cruzi* epimastigote antigens can crossreact with circulating antibodies against all species of *Trypanosoma*. By using generic primers targeting *Trypanosoma* spp. kinetoplast minicircle sequences for PCR analysis of pooled blood DNA samples,

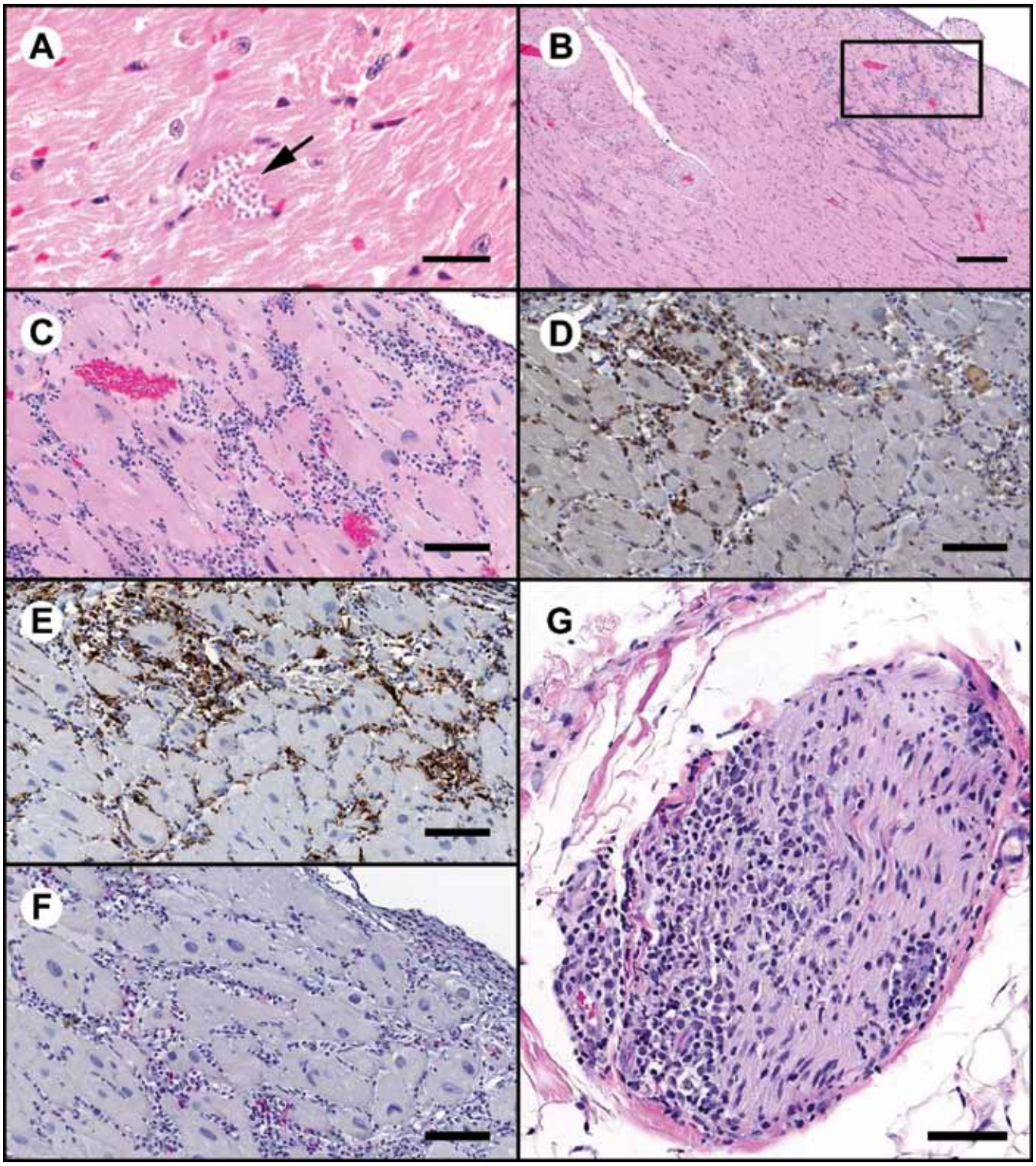

Figure 3. Sections of myocardium demonstrating areas of inflammation and characterization of the inflammatory cell infiltrates by IHC. (A) Cluster of *T. cruzi* amastigotes (arrow). Hematoxylin and eosin stain; bar, 20 µm. (B) Low-power magnification demonstrating moderate to marked subepicardial inflammatory cell infiltrates. Hematoxylin and eosin stain; bar 300µm. The boxed area is shown below. (C) High-power magnification from section in panel B. Inflammatory cell infiltrates are primarily mononuclear cells with fewer neutrophils. Hematoxylin and eosin stain; bar, 100 µm. (D and E) IHC peroxidase procedure with diaminobenzidine chromagen (brown). A considerable proportion of the mononuclear cell infiltrates are positive for (D) CD8 (lymphoid origin) and (E) CD68 (monocyte–macrophage origin). Bar, 100 µm. (F) IHC alkaline phosphatase procedure with Vector red chromagen (red). A small proportion of inflammatory cells are $CD4^+$. Bar, 100 µm. G) Section of nerve at the heart base that is infiltrated by inflammatory cells. Hematoxylin and eosin stain; bar, 80 µm.

we ruled out the presence of nonpathogenic trypanosomes that could give false- positive *T. cruzi* ELISA results. Further characterizing the humoral response, the circulating anti*T. cruzi* IgM ELISA was positive only in newly infected macaques; however, this assay did not achieve sufficient sensitivity in our hands. Even though the present study indicates that *T. cruzi* IgG ELISA

Table 4. Association between *T. cruzi* infection status and anticardiac troponin I level

T. cruzi infection status (IgG and PCR)	Autoantibodies against cardiac troponin I	
	Positive	Negative
Positive	8	35
Negative	0	41

Fisher's exact test of independence, $P = 0.01$.

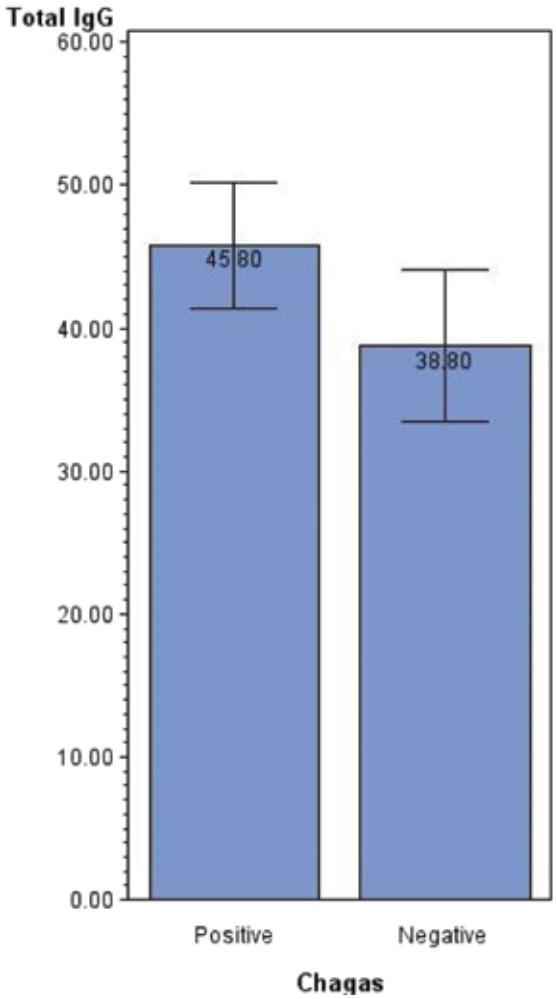

Figure 4. Comparison (mean ± SE, expressed as mg/mL; $P = 0.041$) of total circulating IgG levels in *T. cruzi*-infected and uninfected groups.

alone is adequate for screening for *T. cruzi* infection, further investigation is required to understand the seroconversion kinetics and parasitemia during early infection before ruling out combined screening by using blood-based PCR and serology. In a different study, blood and serum samples collected from 1052 nonhuman primates were screened by using the described ELISA and PCR methodology.[33] Among the 1052 animals tested, 78 were positive for *T. cruzi* by both assays, 102 were positive by ELISA only, and 87 were positive by PCR only. Specifically, 9 animals were PCR-positive but ELISA-negative,[33] underscoring the limitation of serology to detect early infections.

Our interest in screening for *T. cruzi* infection stems from concerns regarding myocarditis and cardiac arrhythmia in infected animals and the effect on pharmaceutical safety studies. In humans, acute Chagas disease is associated with mild cardiac inflammation from mononuclear cell infiltration and can cause death in a small proportion of infected subjects.[27] Chronic Chagas disease can result in progressive, fibrosing cardiomyopathy, resulting in permanent damage.[16] Interestingly, rarely parasites are found in the cardiac tissues of these patients, but *T. cruzi* kinetoplastid and nuclear DNA can be demonstrated readily;[28] this same pattern has been demonstrated in nonhuman primates.[1,9] In the current study, we detected both nuclear and kinetoplastid DNA sequences in the cardiac tissue sections of infected macaques and showed that 6 of 8 animals screened by histopathology had mild to moderate multifocal inflammatory infiltration despite our failure to detect *T. cruzi* pseudocysts or isolated amastigotes in tissues. The cross-sectional nature of this analysis precludes assigning a disease stage (acute compared with chronic Chagas disease) to these cardiac lesions, but given the time frame of introduction to an at-risk outdoor facility, we conclude that macaques infected for less than 24 to 28 mo can present with cardiac inflammation. The inflammatory infiltrate was comprised predominantly of CD8-positive lymphocytes and CD68-positive macrophages with fewer CD4-positive lymphocytes. This finding is consistent with observations made in humans,[14] rhesus monkeys, and mice.[25] In the human study, which was conducted on endomyocardial biopsy specimens, T cells formed 96.3% of the inflammatory infiltrate, with CD8-positive cells forming the predominant cell subpopulation.[13] In *T. cruzi*-infected rhesus monkeys, infiltrating CD68 cells expressed inducible nitric oxide synthase, the levels of which were correlated with the level of loss of connexin43, the major gap junction protein that maintains electrical synchrony in cardiomyocytes.[9] In the same study, using mice deficient in inducible nitric oxide synthase, the authors demonstrated the pivotal role played by the nitric oxide pathway in *T. cruzi*-mediated cardiac injury and conduction abnormality.[9] Furthermore, adoptive transfer studies in mice have shown that infiltrating CD8-positive cells are segregated into interferon γ- positive–perforin-negative and IFNγ-negative– perforin-positive populations, with CD8–perforin double-positive cells associated with worsening of cardiomyopathy, whereas CD8–IFNγ double-positive cells resulted in amelioration of cardiac injury.[24] The role of $CD8^+$ lymphocytes and IFNγ in perpetuating chronic inflammation within the cardiac milieu has been studied in mouse models, in which high percentages of circulating and infiltrating cells in *T. cruzi*-infected C3H mice expressed an activation phenotype characterized by low-signal L-selectin and high-level leukocyte function-associated antigen 1 and very late activation antigen 4.[11] In addition, the study demonstrated high levels of IFNγ-inducible adhesion molecules such as vascular cell adhesion molecule 1 and fibronectin in the cardiac tissue, resulting in intense recruitment and maintenance of activated $CD8^+$ lymphocytes to sustain myocardial injury.[10]

The presence of *T. cruzi* DNA and inflammatory infiltrate in our current study draws attention to the potential for direct parasite-induced damage and *T. cruzi*-specific immune responses, resulting in cardiac inflammation. Other mechanisms might also be involved in facilitating progressive cardiomyopathy. Although not specifically investigated in the current study, we noted marked mononuclear infiltration and damage to the cardiac autonomic ganglia in one infected macaque (Figure 3 G). Cardiac and digestive damage in chronic Chagas disease subsequent to dysautonomia and neuroganglionitis is a well-known phenomenon.[2,6,19] Studies have demonstrated the presence of circulating antimuscarinic and antiadrenergic autoantibodies play a role in mediating or sustaining neuroganglionitis in infected patients.[25,26] Subsequently, we believe that the potential for parasympathetic dysfunction-mediated arrhythmias is a

marked concern in safety pharmacology studies using unscreened and potentially infected cynomolgus macaques.

Another mechanism that is recognized to be important in cardiac inflammation and damage is autoimmunity. The exact mechanism is not well understood, but it is believed to involve the breakdown of peripheral immune tolerance subsequent to initial cardiac damage and leakage of cardiac proteins or as a result of molecular mimicry subsequent to polyclonal activation of B cells during acute *T. cruzi* infection.[3,14] We examined the prevalence of anticardiac protein autoantibodies of the IgG isotype between infected and uninfected groups by using an ELISA specific for anticardiac troponin I. We used cardiac troponin I over other cardiac antigens given the ease of availability of this protein and the scientific effect of such a finding, in light of potential interference with serum troponin I assay function and sensitivity. We identified 8 of 43 (19%) infected animals with high levels of antitroponin I autoantibody titer; this association has not previously been demonstrated in cynomolgus macaques. The pathogenic potential of such a response in driving cardiac inflammation is a subject of active research. For example, in mice, immunization with heat-inactivated *T. cruzi* antigens or inoculation with tissue-culture–derived trypomastigotes triggered the production of autoantibodies and autoreactive immune cells against cardiac antigens.[5] Both methods resulted in cardiac damage, but exposure to heat-inactivated parasite antigen alone was unable to cause tissue inflammation.[5] Our studies are not intended to shed light on the relative contribution of direct parasite-induced damage from autoimmunity as a driver of cardiac inflammation; instead our findings are purely descriptive and require further analysis to validate cardiac troponin autoantibody as a biomarker for the level of cardiac involvement during the course of Chagas disease. In our study, we did not characterize autoreactive cell-mediated immunity; rather we instead hypothesized that cardiac troponin I autoantibody titer might be a surrogate marker of this immunity.

Finally we tried to characterize the polyclonal B cell activation in early *T. cruzi* infection by using a total IgG ELISA assay. *T. cruzi* proline recemase is a B-cell mitogen, and reduction or abrogation of the polyclonal lymphocyte response is associated with resistance to infection and control of tissue pathology.[18] Parasite-specific mitogenic or superantigenic moieties are thought to inhibit the host from mounting a specific immune response.[18] This response potentially might interfere with immunotoxicology endpoints in safety studies, especially those involving active immunization-based endpoints. Although we detected a significant increase in total serum IgG titer in the infected group compared with the uninfected group, the levels did not attain biologic significance. This result may be due to the cross-sectional nature of the study, in which macaques were at different stages of disease, and most were not in the early periods of infection. The fact that we did not find blood PCR-positive but anti*T. cruzi* IgG-negative macaques in this study population strengthens this conclusion.

In summary, we highlight the importance of screening nonhuman primates housed in Chagas-endemic regions for *T. cruzi* infection before the animals are placed on drug safety studies or assigned to breeding activities. This recommendation is based on the infection prevalence rate in south Texas; however, prevalence and incidence could vary depending on housing conditions and regional variations in ecologic risks. Our findings suggest that cynomolgus macaques infected with *T. cruzi* can profoundly affect preclinical cardiac safety profiling of pharmaceuticals by inducing myocardial inflammation and autoimmunity, possibly disrupting cardiac innervations and electrical conduction apparatus and interfering with the measurement of circulating cardiac troponin.

Acknowledgment

We thank Alan Opsahl (Investigative Pathology, Drug Safety R&D, Pfizer) for his help with image processing and editing and the histopathology technical staff (Study Management Group, Drug Safety R&D, Pfizer) for assistance with tissue processing and slide preparation.

References

1. **Andrade MC, Dick EJ Jr, Guardado-Mendoza R, Hohmann ML, Mejido DC, VandeBerg JL, DiCarlo CD, Hubbard GB.** 2009. Nonspecific lymphocytic myocarditis in baboons is associated with *Trypanosoma cruzi* infection. Am J Trop Med Hyg **81:**235–239.
2. **Avila JL.** 1992. Molecular mimicry between *Trypanosoma cruzi* and host nervous tissues. Acta Cient Venez **43:**330–340.
3. **Bermejo DA, Amezcua Vesely MC, Khan M, Acosta Rodriguez EV, Montes CL, Merino MC, Toellner KM, Mohr E, Taylor D, Cunningham AF, Gruppi A.** 2011. *Trypanosoma cruzi* infection induces a massive extrafollicular and follicular splenic B-cell response which is a high source of nonparasite-specific antibodies. Immunology **132:**123–133.
4. **Bern C, Kjos S, Yabsley MJ, Montgomery SP.** 2011. *Trypanosoma cruzi* and Chagas disease in the United States. Clin Microbiol Rev **24:**655–681.
5. **Bonney KM, Taylor JM, Daniels MD, Epting CL, Engman DM.** 2011. Heat-killed *Trypanosoma cruzi* induces acute cardiac damage and polyantigenic autoimmunity. PLoS ONE **6:**e14571.
6. **Bowman NM, Kawai V, Gilman RH, Bocangel C, Galdos-Cardenas G, Cabrera L, Levy MZ, Cornejo del Carpio JG, Delgado F, Rosenthal L, Pinedo-Cancino VV, Steurer F, Seitz AE, Maguire JH, Bern C.** 2011. Autonomic dysfunction and risk factors associated with *Trypanosoma cruzi* infection among children in Arequipa, Peru. Am J Trop Med Hyg **84:**85–90.
7. **Caldas IS, da Matta Guedes PM, Dos Santos FM, de Figueiredo Diniz L, Martins TA, da Silva do Nascimento AF, Azevedo MA, de Lima WG, Neto RM, Torres RM, Talvani A, Bahia MT**. 2012. Myocardial scars correlate with eletrocardiographic changes in chronic *Trypanosoma cruzi* infection for dogs treated with benznidazole. Trop Med Int Health **18:**75–84.
8. **Carvalho CM, Andrade MC, Xavier SS, Mangia RH, Britto CC, Jansen AM, Fernandes O, Lannes-Vieira J, Bonecini-Almeida MG.** 2003. Chronic Chagas disease in rhesus monkeys (*Macaca mulatta*): evaluation of parasitemia, serology, electrocardiography, echocardiography, and radiology. Am J Trop Med Hyg **68:**683–691.
9. **Carvalho CM, Silverio JC, da Silva AA, Pereira IR, Coelho JM, Britto CC, Moreira OC, Marchevsky RS, Xavier SS, Gazzinelli RT, da Gloria Bonecini-Almeida M, Lannes-Vieira J**. 2012. Inducible nitric oxide synthase in heart tissue and nitric oxide in serum of *Trypanosoma cruzi*-infected rhesus monkeys: association with heart injury. PLoS Negl Trop Dis **6:**e1644.
10. **dos Santos PV, Roffe E, Santiago HC, Torres RA, Marino AP, Paiva CN, Silva AA, Gazzinelli RT, Lannes-Vieira J**. 2001. Prevalence of $CD8^+$ αβ T cells in *Trypanosoma cruzi*-elicited myocarditis is associated with acquisition of CD62L(low)LFA1(high)VLA4(high) activation phenotype and expression of IFNγ-inducible adhesion and chemoattractant molecules. Microbes Infect **3:**971–984.
11. **Gottdenker NL, Chaves LF, Calzada JE, Saldana A, Carroll CR**. 2012. Host life history strategy, species diversity, and habitat influence *Trypanosoma cruzi* vector infection in changing landscapes. PLoS Negl Trop Dis **6:**e1884.
12. **Henao-Martinez AF, Schwartz DA, Yang IV.** 2012. Chagasic cardiomyopathy, from acute to chronic: is this mediated by host susceptibility factors? Trans R Soc Trop Med Hyg **106:**521–527.
13. **Higuchi ML, Gutierrez PS, Aiello VD, Palomino S, Bocchi E, Kalil J, Bellotti G, Pileggi F.** 1993. Immunohistochemical characterization of infiltrating cells in human chronic chagasic myocarditis: comparison with myocardial rejection process. Virchows Arch A Pathol Anat Histopathol **423:**157–160.

14. **Leon JS, Daniels MD, Toriello KM, Wang K, Engman DM.** 2004. A cardiac myosin-specific autoimmune response is induced by immunization with *Trypanosoma cruzi* proteins. Infect Immun **72:**3410–3417.
15. **Madrid AM, Quera R, Defilippi C, Defilippi C, Gil LC, Sapunar J, Henriquez A.** 2004. [Gastrointestinal motility disturbances in Chagas disease] Rev Med Chil **132:**939–946. [Article in Spanish].
16. **Molina HA, Kierszenbaum F.** 1989. Interaction of human eosinophils or neutrophils with *Trypanosoma cruzi* in vitro causes bystander cardiac cell damage. Immunology **66:**289–295.
17. **Murcia L, Carrilero B, Munoz-Davila MJ, Thomas MC, Lopez MC, Segovia M**. 2013. Risk factors and primary prevention of congenital Chagas disease in a nonendemic country. Clin Infect Dis **56:**496–502.
18. **Reina-San-Martin B, Degrave W, Rougeot C, Cosson A, Chamond N, Cordeiro-Da-Silva A, Arala-Chaves M, Coutinho A, Minoprio P.** 2000. A B-cell mitogen from a pathogenic trypanosome is a eukaryotic proline racemase. Nat Med **6:**890–897.
19. **Ribeiro Machado MP, Dias da Silva VJ.** 2012. Autonomic neuroimmunomodulation in chagasic cardiomyopathy. Exp Physiol **97:**1151–1160.
20. **Salomon CJ.** 2012. First century of Chagas disease: an overview on novel approaches to nifurtimox and benzonidazole delivery systems. J Pharm Sci **101:**888–894.
21. **Sarkar S, Strutz SE, Frank DM, Rivaldi CL, Sissel B, Sanchez-Cordero V.** 2010. Chagas disease risk in Texas. PLoS Negl Trop Dis **4:**e836.
22. **Shikanai-Yasuda MA, Carvalho NB**. 2012. Oral transmission of Chagas disease. Clin Infect Dis **54:**845–852.
23. **Silva AE, Silva AC, Faleiros AC, Guimaraes CS, Correa RR, Oliveira FA, Correia D, Teixeira AC, Ramirez LE, Teixeira Vde P, dos Reis MA.** 2010. Acute Chagas disease in postrenal transplant and treatment with benzonidazole. Ann Diagn Pathol **14:**199–203.
24. **Silverio JC, Pereira IR, Cipitelli Mda C, Vinagre NF, Rodrigues MM, Gazzinelli RT, Lannes-Vieira J.** 2012. CD8+ T-cells expressing interferon γ or perforin play antagonistic roles in heart injury in experimental *Trypanosoma cruzi*-elicited cardiomyopathy. PLoS Pathog **8:**e1002645.
25. **Sterin-Borda L, Borda E.** 2000. Role of neurotransmitter autoantibodies in the pathogenesis of chagasic peripheral dysautonomia. Ann N Y Acad Sci **917:**273–280.
26. **Talvani A, Rocha MO, Ribeiro AL, Borda E, Sterin-Borda L, Teixeira MM**. 2006. Levels of antiM2 and antiβ1 autoantibodies do not correlate with the degree of heart dysfunction in Chagas heart disease. Microbes Infect **8:**2459–2464.
27. **Tanowitz HB, Kirchhoff LV, Simon D, Morris SA, Weiss LM, Wittner M.** 1992. Chagas disease. Clin Microbiol Rev **5:**400–419.
28. **Tarleton RL, Zhang L, Downs MO.** 1997. 'Autoimmune rejection' of neonatal heart transplants in experimental Chagas disease is a parasite-specific response to infected host tissue. Proc Natl Acad Sci USA **94:**3932–3937.
29. **Toso MA, Vial UF, Galanti N.** 2011. [Oral transmission of Chagas disease] Rev Med Chil **139:**258–266. [Article in Spanish].
30. **Vallejo GA, Guhl F, Chiari E, Macedo AM.** 1999. Species-specific detection of *Trypanosoma cruzi* and *Trypanosoma rangeli* in vector and mammalian hosts by polymerase chain reaction amplification of kinetoplast minicircle DNA. Acta Trop **72:**203–212.
31. **Williams JT, Mubiru JN, Schlabritz-Loutsevitch NE, Rubicz RC, VandeBerg JL, Dick EJ Jr, Hubbard GB.** 2009. Polymerase chain reaction detection of *Trypanosoma cruzi* in *Macaca fascicularis* using archived tissues. Am J Trop Med Hyg **81:**228–234.
32. **Zaniello BA, Kessler DA, Vine KM, Grima KM, Weisenberg SA**. 2012. Seroprevalence of Chagas infection in the donor population. PLoS Negl Trop Dis **6:**e1771.
33. **Zao CL, Burton T, Tomanek L, Rodriguez TH, Nguyen CM, Hurtado-McClure G, Gonzalez-Arroyo S, Carreon MR, Cooke A, Berger R.** 2013. Serological and molecular diagnosis of Chagas disease in captive nonhuman primates in the United States. J Am Assoc Lab Anim Sci **52:**101